Master's Thesis of Science in Agriculture

Generation of intron 22 inversion-based hemophilia A humanized mice and gene correction with Adeno Associated Virus and CjCas9

인트론 22 역위 기반의 인간화 혈우병A 마우스 생산 그리고 아데노부속바이러스와 CjCas9을 활용한 인트론 22 역위 유래 혈우병A의 치료

February 2018

Yoon Hoo Lee

Department of International Agricultural Technology

Graduate School of International Agricultural Technology

Seoul National University

Abstract

Generation of intron 22 inversion-based hemophilia A humanized mice and gene correction with Adeno Associated Virus and CjCas9

Yoon Hoo Lee

Department of International Agricultural Technology

The Graduate School

Seoul National University

Hemophilia A (HA) is caused by mutated *Factor VIII* (*F8*) by nonsense or missense mutation, small indel, splice site mutation, large deletion, or inversion. In particular, intron22 inversion (inv22) derived HA accounts for almost half of patients with severe HA. Despite the need of inversion based mouse model, there have been no suitable inv22 HA mouse model. In this study, I presented genetically induced inversion by using CRISPR/Cas9. In embryo, Non-homologous end joining (NHEJ) mediated inversion was shown at 13.1% efficiency. Homology direct repair (HDR) mediated inversion exhibits 43.8% efficiency, and then, I successfully generated inversion based HA humanized (Hu-inv22 HA) mice at 53.8% efficiency. Despite breakage in flank of inversion junction site, all mutated mouse have inverted *F8*, and human sequence in inversion junction, which I insert in inversion junction for gene correction. I also observed hemophilia A related symptom, such as no detectable *F8* in liver and excessive bleeding. In addition, we revert inverted *F8* in Mouse Embryonic Fibroblast (MEF) by using AAV containing CjCas9 targeting human

sequence in inversion junction. Therefore, we confirmed that AAV can be applicable to correction of the inversion case. The results suggests that Hu-inv22 HA mouse can be used in diverse study for inversion based HA, and additionally AAV can be suitable vector for correction of HA.

Key words : Hemophilia A, Structural variant, inversion, Gene correction, CRISPR/Cas9, Factor8

***Student number*: 2016-20014**

Contents

List of Tables

List of Figures

List of Abbreviations

A.A	Antibiotic, Antimycotic
AAV	Adeno associated virus
B6	C57BL/6
Cas9	CRISPR associated protein9
CjCas9	Campilobacter jejuni Cas9
CRISPR	Clustered regulary short repeat pandrom
crRNA	CRISPR RNA
dKI	double Knock-in
DMEM	Dulbecco modified eagle medium
DSB	Double strand break
ELISA	Enzyme linked immunosorbent assay
F0	Founder
F1	First filial generation
F8	Factor8
FBS	Fetal bovine serum
F8	Factor8
HA	Hemophilia A
hCH	Human chorionic gonadotropin
HDR	Homology directed repeat
Hu-inv22 mouse	intron22 inversion based humanized mouse
IACUC	Institutional animal care and use committee
ICR mouse	Institute of cancer research mouse
int22	intron22
inv22	intron22 inversion
IP injection	Intraperitoneal injection
ITR	Inverted terminal repeat
IV injection	Intravenous injection
KI	Knock-in
LHA	Left homology arm
MEF	Mouse embryoinc fibroblast
MMEJ	Microhomology-mediated end joining
MOI	Multiplicity of infection
MT	Mutant type
NAHR	Non-allelic homologous recombination

NHEJ	Non-homologous end joining
PCR	Polymerase chain reaction
PMSG	Pregnant mare's serum gonadotropin
RGEN	RNA guided engineered nuclease
RHA	Right homolgy arm
sgRNA	Small guide RNA
ssODN	Single strand oligodeoxynucleotide
SV	Structural variant
tracrRNA	Trans acting crRNA
WGS	Whole genome sequencing
WT	Wild type

Introduction

Hemophilia A(HA) is a common bleeding disorder, characterized by hemorrhage and blood clotting problem. HA is genetically X-chromosome linked recessive disorder, while some patients develops HA caused by spontaneous mutation[1]. The estimated incidence of HA is 1:5000 in male. Mutation in *F8* is associated with HA, which is one of the largest gene in human, spanning 191kb, including a 9kb coding region consisting of 26 exons[2, 3]. Many types of gene mutation and genetic recombination in *FactorVIII* (*F8*) gene, including intron22 inversions(Inv22), deletion, insertion, missense, nonsense, and splice site mutation, can cause HA in human.[4] In particular, Inv22 can be spontaneously introduced through non-allelic meiotic recombination between *F8* intron22 and inversely oriented homology region, separated by 319kb distance. Among many types of severe HA, intron22 inversion (Inv22) mutation accounts for over 45% of severe HA patients.[4, 5]

To study HA pre-clinically, several animal model with HA have been generated, including rats[6, 7], dogs[8-10], pigs[11], sheep[12], and mice[13]. All of these animal models were created based on partially deleted or totally deleted *F8* by using genome editing tools. These animal model have been used to study function of each exon, pathophysiology of HA, and effect of therapeutic *F8* treatment depending on Cross Reaction Material(CRM) status. Many studies such as those mentioned above have been conducted regarding HA, but pre-clinical research for HA caused by inversion have been limited, due to lack of the corresponding animal model. Considering distribution of Inv22 case in severe HA, and necessity of pre-clinical study for inv22 HA, it is reasonable to think that inv22 HA animal model is required. However, generation of inv22 animal model is believed to be difficult due to its large size of gene and low incidence of inversion.

Currently, to generate mutated animal model, Clustered Regularly Interspaced Short Palindromic Repeats (CRISPR)/ CRISPR associated protein9(Cas9) have been widely employed. Role of CRISPR/Cas9 is to introduce double strand break (DSB) in DNA. To restore this DNA lesion, intrinsic cell repair pathway called Homology Direct Repair (HDR), Non-Homologous End Joining (NHEJ) is operated. In HDR pathway, broken DNA is repaired based on homologous DNA. This process leads to intact restoration from DNA damage. Using this pathway, donor DNA containing homology can be inserted into break site. In NHEJ pathway, break DNA site is readily rejoined without necessity of homologous DNA. This process results in efficient but error-prone repair from DNA damage. On the basis of these traits, many kinds of Knock-out, Knock-in animal model have been generated. Other than animal modeling based on insertion/deletion, Structural variation (SV) including inversion, duplication, large deletion, translocation also can be facilitated by using CRISPR/Cas9. The first developed tool to induce SV is recombinase mediated rearrangement system like Cre-loxp and Flp-FRT. Subsequent developed tool to facilitate SV is engineered endonuclease system such as TALEN[14], ZFN[15]. All these studies demonstrated that more than two break sites on chromosome can facilitate SV.

As animal modeling using CRISPR/Cas9 have been developed, gene correction methods also notably have been developed. Gene correction can be applied in embryo[16], in vivo[17], or ex vivo level[18]. Genomic aberration can be restored by deleting dysfunctional exon through NHEJ repair[17], or reverting into WT gene through HDR[16]. In embryo, CRISPR/Cas9 can be injected into zygote by using glass micropipette. In vivo, Non-viral vector or viral vector enable delivery of CRISPR/Cas9 into target tissue. Ex vivo, patient derived cell can be corrected using

CRISPR/Cas9, followed by transplantation into the cell owner. Among several methods, viral vector is thought to be efficient in vivo transduction tool. In particular, one of viral vector, Adeno Associated Virus (AAV), is believed to be promising vector for gene correction. Because the vector is non-pathogenic, and can infect efficiently both non-dividing cell and dividing cell for long term[19-22]. The vector also has minimal host immune response, compared to other viral vectors. Although AAV has limit to apply in gene editing due to its 4.9 kb packaging size, CjCas9 (2.9kb) can overcome packaging limit and be packed with sgRNA in single AAV[23].

To treat HA, classic therapeutic strategy is directly infusing F8 protein into patients. This protein injection was proven to enable ameliorate bleeding phenotype relatively for a long term[24, 25]. Despite the efficacy of the protein based therapy in HA, there are several limitations. First, F8 has short half-life, requiring repeat protein infusion. Moreover, it is estimated that 80% of patients worldwide are unable to receive this treatment, due to the high cost[26]. Above all, one of the major hindrance of F8 protein treatment is occurrence of anti-F8 antibody called inhibitor. 15% of inv22 *F8*patients, who was treated with F8protein, developed clinically relevant inhibitor[5]. To avoid inhibitor development, gene therapy to treat Hemophilia B, which has similar coagulation disorder, was investigated. The study shows that AAV is efficient delivery tools, and just 1-6% increase of FIX level improves disease phenotype for a long term[27].

In this study, I generated mouse with human target sequence knock in and simultaneous inversion on *F8* gene, and evaluated the efficiency of gene targeting, hemophilia A phenotype and possibility of in vivo gene correction with adeno-associated virus. Taken together, I want to elucidate the proof of concept about in vivo gene therapy especially for HA.

Method

Design for sgRNA, ssODN

De novo inv22 in HA occurs due to homology between *F8* intron22 and outside *F8* region, separated by 319kb from intron22 (hereinafter I will refer this region as distal22). To imitate inversion, introduction of concurrent DSB using multiple sgRNA was employed[14]. In silico, I chose 10 sgRNA binding site candidates for each region by using RNA guided engineered nucleases (RGEN) online tool (www.rgenome.net) (Table 1). To assess cleavage ability of each sgRNA, Each sgRNA with Cas9 protein were transfected into NIH3T3 cells by using Neon electroporator(Thermo Fisher Scientific, Waltham, MA, USA). Then, the cells were harvested after 48 h incubation, and DNA was extracted and deep sequencing was conducted on PCR amplicon by using MiSeq (Illumina, San Diego, CA, USA). Indel ratio of amplified target region was analyzed by online Cas-Analyzer.

In addition, I designed 2 single strand oligodeoxynucleotides (ssODNs) to induce inversion and human target sequence dual knock in. Once concurrent DSB occur, large chromosomal segment will arise, and this segment will be re-joined in inverted manner or non-inverted manner. To guide this chromosomal segment in inverted orientation, we designed ssODN, which consist of 70bp left homology arm (LHA) containing the end of the excised chromosome region, and 70bp right homology arm (RHA) containing the opposite the end of the excised chromosomal region. In addition, 60bp of pre-screened CjCas9 target sequence for human intron22 and distal region was also added in the middle of the ssODN as the future target region for re-inversion mediated gene correction . Brief strategy for simultaneous inversion and dual knock is shown in figure 1, and detail ssODN sequence was in Table 2. ssODNs were synthesized with commercial service (IDT, San Jose, CA, USA)

Table 1. Selected candidate sgRNA binding site for int22 and distal region for inversion

Target	No.	sequence of sgRNA binding site (5' to 3')	Mismatch		
			0 bp	1 bp	2 bp
mF8-int22	int22-Sp1	GTGGCCTGGTCAAGCTTATC	1	0	0
	int22-Sp2	TCATGGTGGAAGCCGTGGCC	1	0	0
	int22-Sp3	TGGCTTCATGGTGGAAGCCG	1	0	0
	int22-Sp4	TTTGCAGAACAATCCCCTTT	1	0	0
	int22-Sp5	TCTGCAAAATTGAAGAACTC	1	0	0
	int22-Sp6	GAAGAACTCTGGACTTACTA	1	0	0
	int22-Sp7	TTACTAAGGGCTGAACAAGG	1	0	0
	int22-Sp8	CAATAGCCAGTATGTGGCCG	1	0	0
	int22-Sp9	CTCGGCCACATACTGGCTAT	1	0	0
	int22-Sp10	TCGGCCACATACTGGCTATT	1	0	0
mF8-distal	distal-Sp1	AGCGGGGCTAACACTGCACA	1	0	0
	distal-Sp2	TGAAGGCTTAAAGCAGAAGC	1	0	0
	distal-Sp3	GCATACGGGTCAGATGCCTG	1	0	0
	distal-Sp4	GGCATACGGGTCAGATGCCT	1	0	0
	distal-Sp5	GGGCATACGGGTCAGATGCC	1	0	0
	distal-Sp6	CCCGTATGCCCTGCCGTATT	1	0	0
	distal-Sp7	CCAAATACGGCAGGGCATAC	1	0	0
	distal-Sp8	TGGCACAACCAAATACGGCA	1	0	0
	distal-Sp9	CTGGCACAACCAAATACGGC	1	0	0
	distal-Sp10	CACTGTCTGGTAAGAGGTGC	1	0	0

Table 2. ssODN sequence of int22 and distal region

	ssODN sequence (5' to 3')
Int22 region	ACACCATCTCACTGGGTGCCATGGAACCACCCCTCATCCAAACACACCATTTGGCCAGTGACTTCCAGATGGCATCTGGGGACG GCAGAGGGTATCACACGGCTGAACGTTACCAGCACCCCGAGAACACACAAGGTACAAACTAAAGGTCCCAAGAGGGACCTTAC TGAAAAGTTATTGAATTTAAAGAACAATATAAG
Distal region	TTGTTCTATTAACCCAGGTTCATTAACATAAAAATAGCATTGTTCCCCCAGTACAACACAAGTACCTCCTGTGTTCTCGGGGTGC TGGTAACGTTCAGCCGTGTGATACCCTCTGCCGTCCCCAGATGCCTGCCCTGCCGTATTTGGTTGTGCCAGCACCTCTTACCAGA CAGTGATCTGAGGACTCAGTGGACCCAGAT

Pupple letters: LHA intron22, red letters: human target sequence, green letter: LHA-distal22, Blue letter: RHA-intron22, yellow letter: RHA distal 22

In vitro transcription

For concurrent DSB, 3ea sgRNA was selected among 10ea sgRNA candidate for each target region. For synthesizing Cas9 mRNA and sgRNA, we applied conventional PCR based *in vitro* RNA synthesis method. To synthesize Cas9 mRNA, first, we have Cas9 plasmid (Plasmid #43945) linearized by using XbaI restriction enzyme, and then, T7 reaction was conducted on linearized template by using mMESSAGE mMACHINE kits (Thermo Fisher Scientific). To synthesize sgRNA, dimer formation based PCR by annealing 15 bp overlapped crRNA and tracrRNA was conducted. PCR condition was 95°C 30 sec, 35 cycles of 95°C 30 sec, 55°C 30 sec, 72°C 30 sec, and final polymerization in 72°C 5 min. Annealing product was subject to template for sgRNA synthesis. Synthesis and purification of sgRNA were conducted by using Megashortscript T7 kit (Thermo Fisher Scientific), and MEGA clear kit (Thermo Fisher Scientific) respectively. All procedure was carried out following the manufacturer's instruction.

Microinjection

For collecting 1 cell embryos, C57BL/6 female mice were injected with 5 IU of PMSG(Prospec Bio, East Brunswick, NJ, USA) to induce the growth of follicles by ovaries, followed by super-ovulation through IP injection of 5 IU of hCG(Prospec Bio). Next day, embryos were collected from oviduct, and incubated at 37°C with 5%O_2, 5%CO_2 in KSOM media for 2hours. To induce high DSB in each target region, DSB formation efficiency of cas9 mRNA and protein was assessed in 25 embryos in each group. Next, efficiency of ssODN mediated inversion was examined in embryo. *In vitro* analysis for DSB and inversion efficiency was conducted with cultured morula or blastocyst and PCR based method. Finally, 50ng/μl of Cas9 mRNA, 30ng/μg of each sgRNA, and 20ng/μl of each ssODN were

microinjected into pronucleus of C57BL/6 embryos. After culture for overnight, 2-cell embryos were transplanted into oviduct of ICR surrogate dams. Animal experiment was approved by institutional animal care and use committee (IACUC) of Seoul National University, and conducted IACUC guidance.

Genotyping and sequencing

Genotyping was conducted with DNA from toe-clip, and PCR based genotyping was conducted. Primers for WT, inversion, inversion/KI, large deletion, duplication were designed respectively. Two regions are amplified to determine genetic arrangement. One is *F8* intron22 region, another is outside the *F8* gene, 319kb distanced from intron22. Both regions are sgRNA target site. Pair of #1,#2 and #3,#4 primer are designed to determine WT(Figure 1). Pair of #5,#6 and #7,#8 primer are designed to determine inversion. 4 pairs of primers were designed to determine inversion/KI, which detect human sequence, we inserted in the middle of ssODN. Outside and inside of inversion/KI were designed respectively to detect expectedly complex inversion foam. Primer #17,#18, Primers for large deletion, were located on flank of target region, so that only large deletion foam can be detected, because amplified length(319kb) in intact WT is too big to be amplified. Brief primer design and sequence was shown in table 3 and figure 2.

After founder production, additional quantitative PCR (qPCR) was conducted for detecting structural variation such as duplication by direct comparison of target sequence amplification level. Four pairs of duplication primers were selected from Primer bank(http://pga.mgh.harvard.edu/primerbank/index.html; [28], two of which are located on inside of inverted region(*F8, Brcc3*), and the others are located on outside of inverted region(*Tlr7, Abcd1*). Primer information for qPCR is in table 4.
To confirm human sequence knock in into precise target site, PCR amplicon of

target region was sequenced. Briefly, amplicon was purified by PCR purification kit (Qiagen, Hilden, Germany) and gel extraction kit (NEB, Hichin , UK). After TA cloning with commercial kit (Thermo) sanger sequencing was conducted. With alignment with reference, inversion and dual human sequence knock in was confirmed.

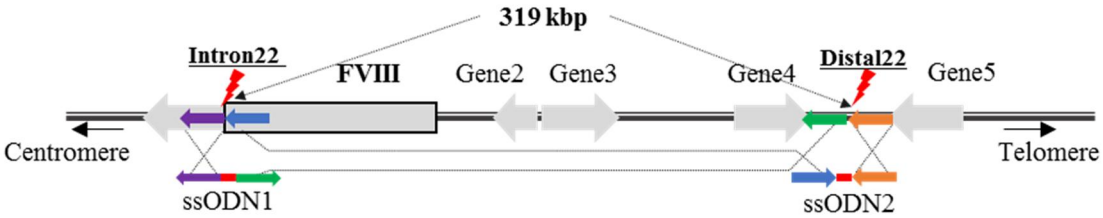

Figure 1. Brief schematic for inversion and dual knock in based HA model mouse generation. SgRNAs for 2 target sites were selected (red thunder shaped symbol, and distance between 2 site is approximately 319 kbps. Indeed, specific ssODNs were designed for inversion and human sequence knock in. In case of int22 target site, 70 bp of external homology sequence, 60 bp of human sequence, and 70 bp of complementary sequence of distal internal were designed.

Table 3. Sequence of primers for genotyping

		Size (bp)	Primer. No	Sequence Fwd (5' to 3')	Tm (°C)	Primer. No	Sequence Rev (5' to 3')	Tm (°C)
F8_Int22	WT	395	1	5’-ACCACCCCTCATCCAAAC-3’	59	2	5’-AGAAGAGTCCCAATAGCCAG-3’	59
	Inv	512	5	5’-CTTTCCTTCCCAACTGCTTCT-3'	60	6	5’-CCATTCACCTTTTTCTCCACC-3’	60
	dKI-Inv inside	344	9	5’-TACCAGCACCCCGAGAACA-3'	59	10	5’-CCTCCATTCACCTTTTTCTCC-3’	59
	dKI-inv outside	688	11	5’-TCCCCTCTCCCCACTTTCT-3’	60	12	5’-TGTGATACCCTCTGCCGTC-3’	60
Distal	WT	762	3	5’-CTTCCTCCATTCACCTTTTTCT-3'	59	4	5’-ACTACTTTTCGGCACACCTT-3’	59
	Inv	778	7	5’-TTTCAGTCCCACAGCTCCTT-3'	60	8	5’-ACTACTTTTCGGCACACCTT-3’	59
	dKI-Inv inside	420	15	5’-CATTTCAGTCCCACAGCTCC-3'	60	16	5’-TACCAGCACCCCGAGAACA-3’	59
	dKI-inv outside	536	13	5’-TGGTAACGTTCAGCCGTG-3’	59	14	5’-GGCCAGGAGAAACAGCAA-3’	59
Large Deletion		1,269	17	5'-AGAGGGGGCTGAAAGAAAAGA-3'	60	18	5'-AAAAAGGGAGAAGAAGGGGGA-3'	59

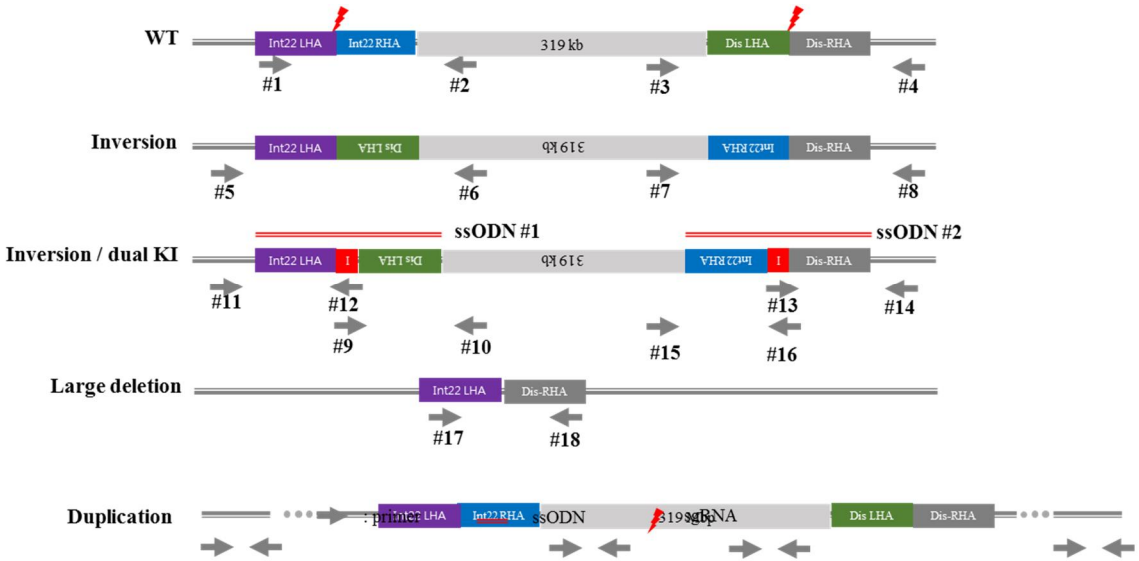

Figure 2. Genetic location of designated primers. To distinguish wild type, inversion/dual knock in and large deletion, 14 primers were designed. Each arrow indicate primer.

Table 4. Primer sequences for quantitative PCR

	Gene	Size (bp)	PrimerBank.ID	Sequence Fwd (5' to 3')	Tm	Sequence Rev (5' to 3')	Tm(°C)
Inverted region	*F8*	128	6679733a1	ATGCAAATAGCACTCTTCGCT	60.1	ACACTGAGCAGATCACTCTGA	60.2
	Brcc3	101	22165366a1	GTGCAGGCGGTTCATCTTGA	62.8	AACTCCCCTATACACAGACCC	60
Outside of Inverted region	*Tlr7*	207	18875360a1	ATGTGGACACGGAAGAGACAA	61.1	GGTAAGGGTAAGATTGGTGGTG	60
	Abcd1	180	6671497a1	AAATCTACCCTCTAGTACGGCAG	60.7	TTTCCCGGCACAAGACTCG	62.2
Housekeeping Control	*Gapdh*	123	6679937a1	AGGTCGGTGTGAACGGATTT	61	TGTAGACCATGAGTTGAGGTCA	61

Whole genome sequencing

Although we determined Inv22 MT mice by genotyping using standard PCR based method, complicate *de novo* genomic rearrangement hamper its precise interpretation. Moreover, many repeat sequence, high GC content, and duplicons in *F8* hinder characterization of genomic rearrangement by PCR based approaches. Owing to these challenges, we conducted whole genome sequencing (WGS) on the mutant mice, pre-determined by PCR based method. This analysis helps concrete inv22 event in mice, and identify occurrence of any other genomic rearrangement. gDNA, extracted from Inv22 mouse tail tissue was used, and WGS was performed by Teragen (Seoul, Korea).

Germ line transmission analysis and model animal production

After confirming founder mouse, germline inheritance was confirmed by breeding. Owing to characteristic of X-liked recessive disorder, it is impossible for obtaining hemizygous male in F1 generation, while it is possible to get HA carrier female mice in F1 generation. For the ease of later experiments, we only used hemizygous male mice. To obtain hemizygous male mice, two consecutive mating was carried out. Hemizygous male in F0 generation were bred with WT B6 female, and heterozygote females in F1 generation were bred with WT B6 male (Figure 3).

In general, heterozygous HA carrier has 50% of residual plasmatic F8 activity, and normally manifest mild HA[29]. However, severe HA in heterozygous females is also rarely observed. It may be explained by coexistence of skewed Lyonization (biased X-chromosome inactivation) and the heterozygous carrier condition[30].

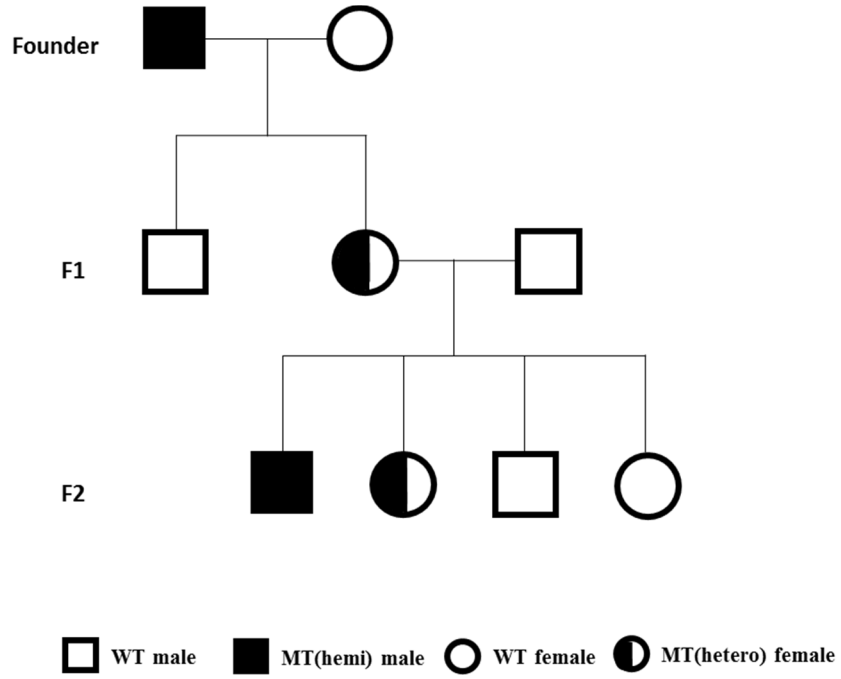

Figure 3. Breeding strategy for hemophilia A mouse production. To product hemizygote male mouse, breeding was conducted with wild type male and heterozygote female mutant mouse, and 50% of male pups were hemizygote mutant male.

In vivo bleeding test

To identify clotting disorder caused by hemophilia A, *in vivo* bleeding test was conducted by measuring blood loss by transecting distal tail with minor modification from previous report[31]. Briefly, mice were anesthetized via intra-peritoneal (IP) injection by avertin, then,1cm from distal tail end was cut. Then, blood was collected for 30 minutes, and weight of blood was normalized with body (mg/g). Clotting disorder was confirmed by comparison between normal and hemophilia phenotype.

AAV-CjCas9 design for re-inversion

In order to develop re-inversion mediated gene correction, *Campylobacter jejuni* cas9 (CjCas9) based sgRNA was designed for human target sequence. In case of human *F8* inversion patient, inversion was developed by highly homology sequence, thus sequence of int22 and distal were similar or almost same. In other word, single target CRISPR/cas9 could be useful for each target site. As described above, prescreened and evaluated human target sgRNA binding site sequences were knock-in into mouse *F8* int22 and distal region which were 319 kbs distance. Two different human target sequence was intorducted as Cj12: 5'-GGCATCTGGGGACGGCAG AGGGTATCACAC-3'. Cj30 : 5'-GGCTGAACGTTACCAGCACCCCGAGAAC AC-3'. CRISPR vector for gene targeting included CjCas9 regulated under ubiquitous promoter regulation, and sgRNA regulated under U6 promoter. Due to vector size is about 3.9 kb, AAV could be used for packing. Vector map was shown in Figure 4, and strategy for re-inversion was exhibited in Figure 5. After considering specific tropism in liver[32], adeno associated virus type 6 was selected for in vivo CRISPR/Cas9 transduction, and viral particle was prepared by Vector Biolabs (Malvern, PA, USA) and Vigene (Rockville, MD, USA). AAV for introducing re-inversion : AAV-CjCas9-Cj12 was produced at titer of 1.20~1.44 x

10^{13} vg/ml, AAV-CjCas9-Cj30 was produced at titer of 1.90 x 10^{13} vg/ml, and AAV-control containing only CjCas9 : AAV-Cjonly was produced at titer of 3.37 x 10^{13}vg/ml.

In vitro AAV transduction for evaluation of re-inversion efficiency

To validate NHEJ dependent genetic rearrangement of founder mouse, in vitro AAV transduction was conducted with mouse embryonic fibroblast (MEF) cell. For MEF preparation, heterozygote Hu-Inv22 female mouse was mated with wild type male, and female was sacrificed at 14 pregnant days and fetus were aseptically obtained. After classical primary culture procedure as chopping, digesting with protein kinase and plating, MEF cell were cultured at 37°C with CO_2 in DMEM supplemented with A.A and FBS. Genomic DNA was extracted from each fetus derived MEF, and genotyping was conducted with specific primer (table 3). By analysis DNA amplification pattern, mutant versus wild type, and male versus female was identified.

Next, *in vitro* AAV transduction was performed. Briefly, 3x10^4 MEF cells were culture in 4 well dish, and AAV transduction was conducted after 24h. For AAV transduction, culture medium was removed from each well, and 4~10 x 10^6 MOI of AAV were added in target well. After 2 hour AAV transduction, culture medium was re-filled into each well. In this study, 3 type of AAVs were applied as AAV-CjCas9-Cj12, AAV-CjCas9-Cj30, and AAV-CjCas9. Two after AAV transduction, cell were harvested, and genotyping with wild type control PCR primers was conducted for confirmation of CjCas9 and NHEJ mediated re-inversion. Brief information about procedure and viral solution for *in vitro* AAV transduction was shown in figure 6 and table 5.

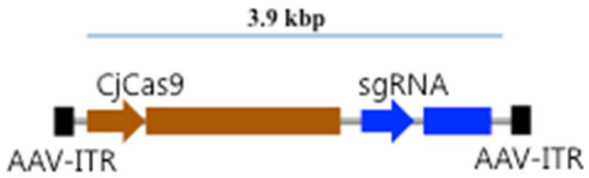

Figure 4. Structure map of AAV-CjCas9-sgRNA. For preparation AAV6 mediated all-in-one type CjCas9, promoter for CjCas9 gene and sgRNAs were inserted between ITR sequences.

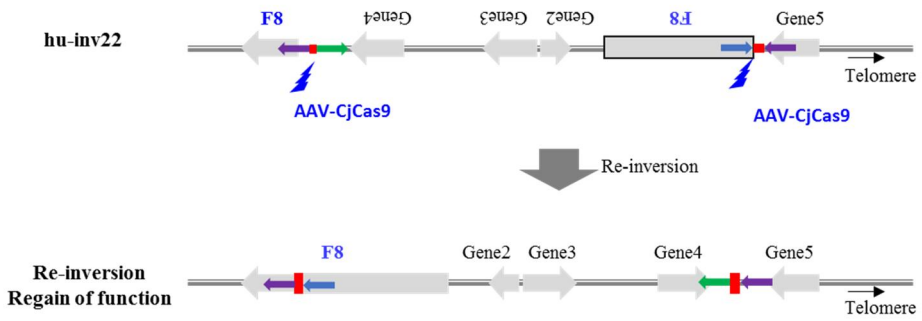

Figure 5. Brief strategy for in vivo gene targeting. With DSB inducing in both target site (red box) by AAV-CjCas9, *F8* inversion would show re-inversion.

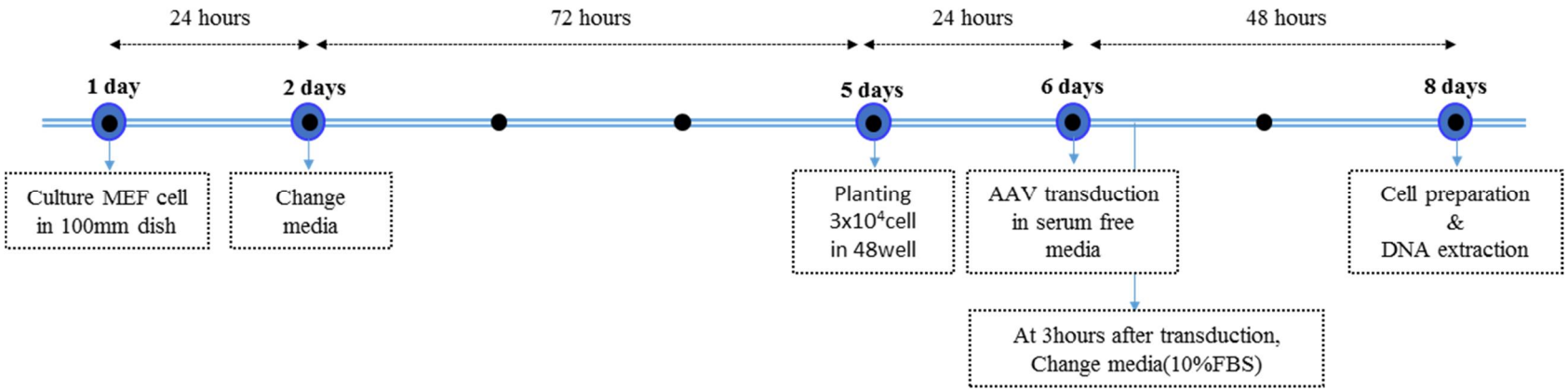

Figure 6. **Brief procedure for *in vitro* AAV transduction** *in vitro* AAV transduction was carried out, following above schedule. MEF cells were obtained from female MT mouse in F1 generation. AAV was treated at 4~10 x 10^6 MOI. At 2days after transduction, MEF cells were collected. AAV treatment causative re-inversion was determined by using PCR & sequencing.

No.	AAV type	Maker	Virus (vg/ml)	MOI	Media
1	AAV-CjCas9-Cj12	Vectorbiolabs	1.44×10^{13}	4.32×10^{6}	DMEM197+virus mix 3ul
2	AAV-CjCas9-Cj30	Vectorbiolabs	1.90×10^{13}	5.7×10^{6}	DMEM197+virus mix 3ul
3	AAV-CjCas9 (control)	Vigene	3.37×10^{13}	10.1×10^{6}	DMEM197+virus mix 3ul

Table 5. **Brief information about *in vitro* AAV transduction** To evaluate *in vitro* re-inversion, two AAV-CjCas9-sgRNA vector were used. AAV-CjCas9 vector was treated as control. AAV was administrated at 4~10 $\times 10^{6}$ MOI.

In vivo AAV transduction and phenotype evaluation

To validate *in vivo* gene correction by NHEJ mediated re-inversion, AAV with Cjcas9-sgRNA was injected into the mutant mouse. Total 20 mutant male mice were randomly divided, 2.88 x 10^{11}vp of AAV-target (AAV-CjCas9-Cj12) and AAV-control (AAV-CjCas9) were injected via intravenous (IV) route. Brief information about viral solution was shown in table 6.

To see *in vivo* transduction causative phenotype change, bleeding test, ELISA and immune-histological examination on AAV treated hu-Inv22 mice was conducted at 4-9weeks after injection. F8 protein derived from Structural variant (SV) can be defective in the expression, secretion, or protein stability in circulation, which leads to different F8 protein level in circulation. To measure plasmatic F8 protein level, ELISA was conducted with F8 ELISA Kit (Mybiosource, San Diego, CA, USA) as manufacturer's introduction.

Vector	Manufacture	Titer	Injection Volume (per head)	Prepared Volume (in total)
AAV6-Cj12(target)	Vector Biolabs	1.20 x 10^{13}vg/ml	Stock 24ul + Saline 176ul	Stock 204ul + Saline 1496ul
AAV6-Cjonly(control)	Vigene	3.37 x 10^{13}vg/ml	Stock 8.6ul + Saline 191.4ul	Stock 64.5ul + Saline 1435.5ul

Table 6. Strategy for *in vivo* AAV transduction To adjust amount of administrated virus particle (VP), calculated AAV volume was mixed in saline. 2.88x10^{11} VP in 200ul saline was infused into mouse via intravenous route.

Results

Selection of sgRNAs with high DNA cleavage potential

At first, 10 sgRNA binding candidate sites were selected and deep-sequencing based DNA cleavage activity was assessed in NIH3T3 cell line. As shown in figure 7, candidate target sgRNA of 3 site in intron22 region and 5 site in distal region showed DSB inducing activity. Overall DSB inducing potential is high in the intron22 region than distal region. Based on the each DSB potential, 3 sgRNA binding site was selected (intron22 region: 5'-GTGGCCTGGTCAAGCTTATC TGG-3', 5'- TTTGCAGAACAATCCCCTTTGGG-3' and 5'-TTACTAAGGGCTG AACAAGGAGG-3', distal region: 5'-AGCGGGGCTAACACTGCACAAGG-3', 5'-GCATACGGGTCAGATGCCTGGGG-3' and 5'-CCAAATACGGCAGGGCA TACGGG-3'), and some of them were located in overlapping site. It is assumed that if eyery sgRNAs showed DSB, there is about 124 bp sized deletion in intron22 region, and 115 bp deletion in distal region. Detail sequence of sgRNAs were shown in table 7. After confirming sgRNAs, ssODN for human sequence insertion and enhancing inversion was designed. Due to expected deletion by selected sgRNAs, homology sequence of ssODN was modified (Figure 2).

High DNA cleavage potential of cas9 mRNA

High efficiency of DSB formation is important for developing chromosomal rearrangement based inversion. Thus, we want to compare the DNA cleavage efficiency of protein and mRNA. Protein type cas9 could fuse with sgRNA and it could DSB potential after transfection into embryo, but mRNA type cas9 should be translated to protein for having activity. Even though it is not significantly different, overall DSB formation potential seemed to be high in cas9 mRNA test than cas9

protein. In mRNA injected embryo, there was 33% DSB in intron22 region, and 100% of DSB in distal region (Figure8).

HDR mediated inversion/ NHEJ mediated inversion

According to DNA repair pathway, almost of DSB developed to non-homologous end joining (NHEJ). However, we assumed that dual DSB with guiding ssODN could develope inversion type structural variation. However, there was also possibility of simple NHEJ mediated inversion. To verify inversion developing efficiency, additional microinjection and evaluation analysis was conducted. Briefly, in SpCas9-sgRNA complex mediated dual DSB, only 13% of embryos exhibited inversion specific genotyping result, but addition of ssODN improved the inversion efficiency up to 43.8% (7/16). In other word, inversion rate increased almost 3 folds when target site was guided by ssODN (Figure 9). This result indicate that ssODN might be essential for DSB induced structural rearrangement.

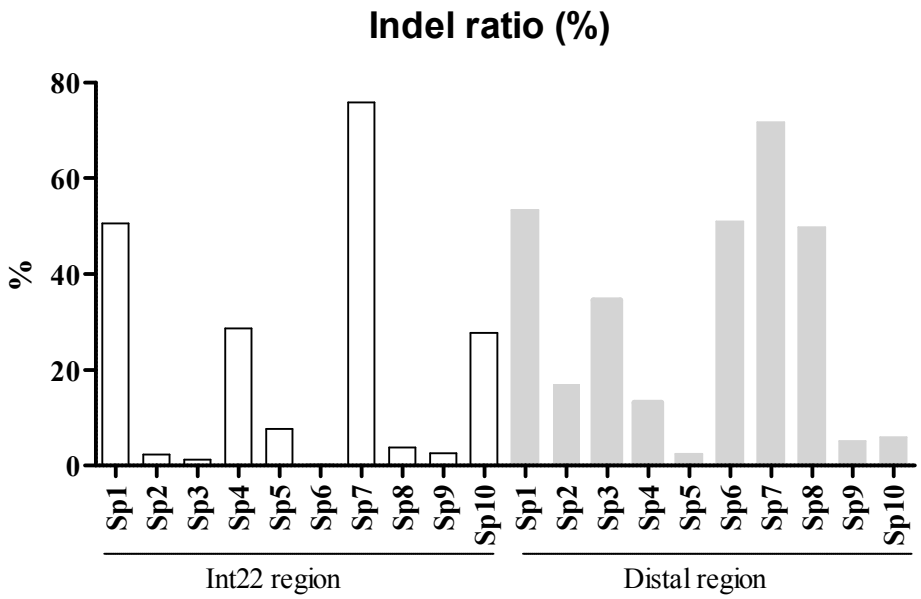

Figure 7. **Cleavage ability of target sgRNA** . Indel ratio was assessed by using RGEN Cas-Analyzer. 3 out of 10 sgRNA were selected for intron22, distal22 respectively, based on indel efficiency.

A

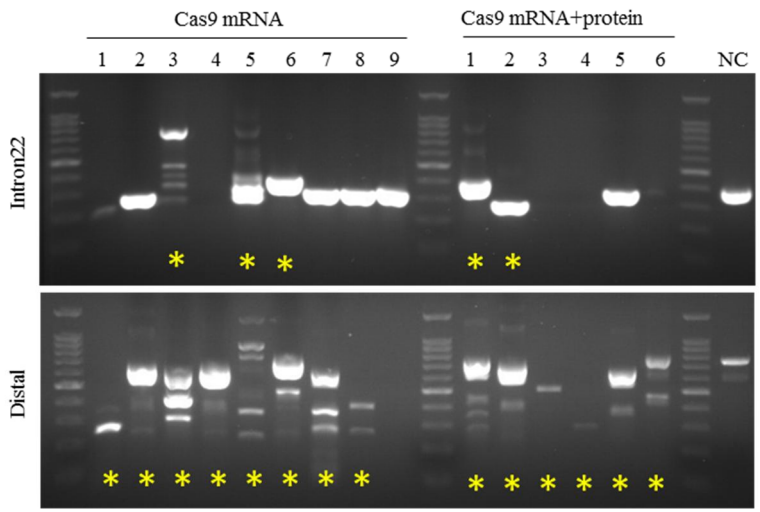

B

	No. of embryo	No. survive embryo (%)	No. of blastocyst (%)	Mutation rate (%) (No. of indel / BL) In **Int22**	Mutation rate (%) (No. of indel / BL) In **Distal**
Cas9 mRNA	25	20 (80)	9 (45)	33.3 (3/9)	77.7 (7/9)
Cas9 mRNA/protein	25	22 (88)	6 (27)	33.3 (2/6)	100 (6/6)

Figure 8. Comparison of DNA cleavage potential between cas9 mRNA and protein. Total 50 embryo was randomly divided, and half of them were microinjected SpCas9 mRNA and sgRNAs, and the others were microinjected protein form SpCas9 and sgRNA. A Yellow symbol indicate accurate DSB and inducing NHEJ.

Gene	No.	RGEN Target	More than minimum frequency	Insertions	Deletions	Indel ratio (%)
Int22	int22-Sp1	GTGGCCTGGTCAAGCTTATC	49193	3140	21745	50.60%
	int22-Sp2	TCATGGTGGAAGCCGTGGCC	43112	256	753	2.30%
	int22-Sp3	TGGCTTCATGGTGGAAGCCG	54414	0	697	1.30%
	int22-Sp4	TTTGCAGAACAATCCCCTTT	45573	3101	9969	28.70%
	int22-Sp5	TCTGCAAAATTGAAGAACTC	44050	738	2675	7.70%
	int22-Sp6	GAAGAACTCTGGACTTACTA	48685	18	63	0.20%
	int22-Sp7	TTACTAAGGGCTGAACAAGG	34063	12944	12905	75.90%
	int22-Sp8	CAATAGCCAGTATGTGGCCG	54191	295	1782	3.80%
	int22-Sp9	CTCGGCCACATACTGGCTAT	55772	699	766	2.60%
	int22-Sp10	TCGGCCACATACTGGCTATT	49599	5166	8567	27.70%
Distal	distal-Sp1	AGCGGGGCTAACACTGCACA	28811	5080	10317	53.40%
	distal-Sp2	TGAAGGCTTAAAGCAGAAGC	23953	877	3160	16.90%
	distal-Sp3	GCATACGGGTCAGATGCCTG	26023	2278	6688	34.50%
	distal-Sp4	GGCATACGGGTCAGATGCCT	24522	108	3114	13.10%
	distal-Sp5	GGGCATACGGGTCAGATGCC	26958	121	527	2.40%
	distal-Sp6	CCCGTATGCCCTGCCGTATT	23065	3360	8404	51.00%
	distal-Sp7	CCAAATACGGCAGGGCATAC	25550	9775	8536	71.70%
	distal-Sp8	TGGCACAACCAAATACGGCA	25188	2348	10194	49.80%
	distal-Sp9	CTGGCACAACCAAATACGGC	19692	387	639	5.20%
	distal-Sp10	CACTGTCTGGTAAGAGGTGC	26228	140	1396	5.90%

Table 7. Sequence, DSB acitivity of sgRNA candidate on *F8* intron22 and distal region

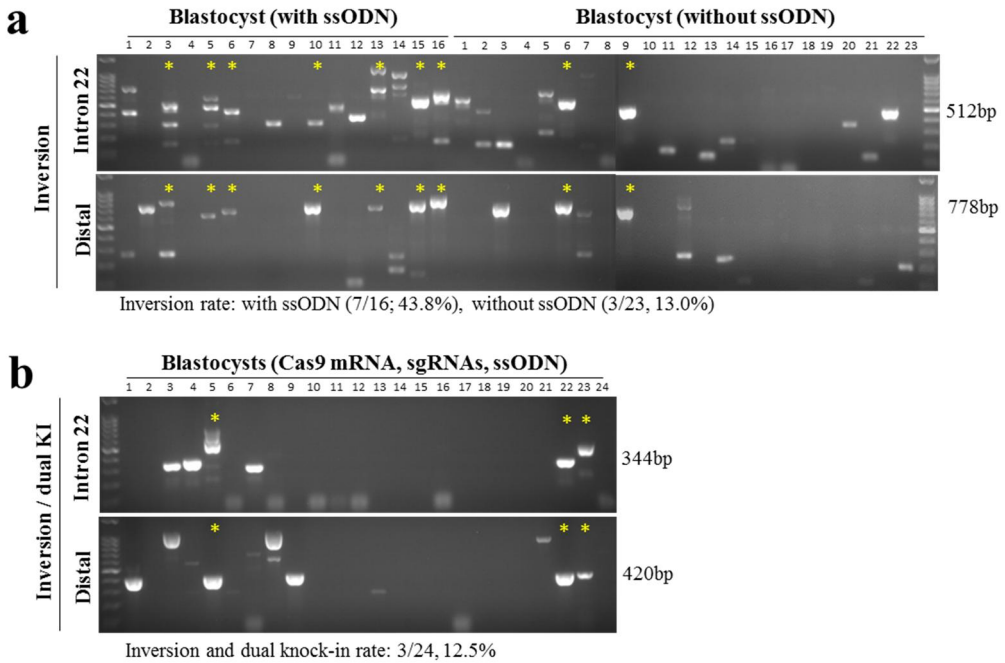

Figure 9. Comparison between HDR mediated inversion and NHEJ mediated inversion. Microinjection was conducted into 1 cell embryo with or without ssODNs was conducted. Yellow symbol indicate target band for inversion. In the ssODN absent group, three times high inversion ratio was shown (Figure 9.a). To find out human sequence KI at two inversion break site, genotyping was conducted by using appropriate primers. Briefly, 12.5% of inversion with dual KI was found in microinjected embryos.

Successful Generation of dual knock in and inversion mediated Hemophilia A model mouse

After setting up optimal condition for microinjection, 324 embryos were microinjected in one cell stage, and 250 viable embryo were transferred to surrogate ICR dam. Total 20 pups were produced, but 10 pups were cannibalized by their foster mother, so only 10 pups were survived after birth. Overall birth rate is 8% and it was relatively lower than our expectation. Genomic DNA were extracted from 10 live pups and 3 dead pups. Genotyping results revealed that 30.1% (4/13) of pups were successfully established as inversion and dual knock in, and there there were 2 pups with inversion and single KI (#11 and #12 pups) and with large deletion (#9 pups with 319 kbp deletion) (Figure 10 and Table 8)

Deep analysis for F0 with inversion/dKI revealed that all F0 showed precise KI in single region, but also showed DNA fragment breakage in opposite region (Fig. 11). The cause of DNA fragment breakage is still uncertain. However, every F0 showed simultaneous inversion and dKI with human target sequence, and they are valuable for *in vivo* gene therapy model for human.

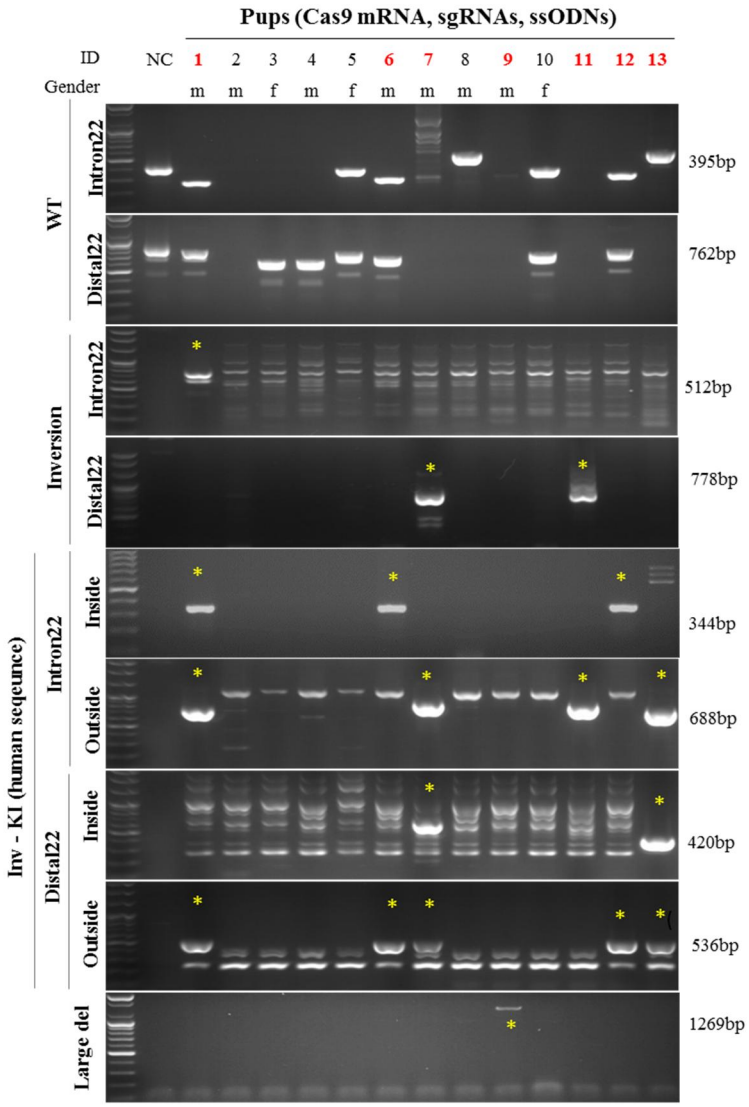

Figure 10. Genotyping for produced 13 pups. For genotyping 9 type of PCR condition was conducted. Yellow symbol indicated positive band for each PCR condition, and red letter indicated presumed founder pups with inversion/dual knock in or large deletion. Overall, 7 out of 13 pups were identified as mutant. Inversion was found in 6 pups (line1, line6, line7, line11, line12, line13), and deletion was found in 1 pup (line9). Among inversion mouse, 3 pups (line11, 12, 13) were dead after birth.

Table 8. **Summary of *F8* inversion/dual knock in mouse generation**

Target gene	No. of injected embryo	No. of 2 cell stage embryo (%)	No. of blastocyst (%)	No. of transferred embryos	No. of offspring (%)	Mutation ration (%) (No. of inversion/total blastocysts or offsprings)
F8	**34**	**26 (76)**	**16 (57)**	**NA**	**NA**	**43.8 (7/16)**
	324	**307 (94)**	**NA**	**250**	**20 (8)**	**53.8 (7/13)**

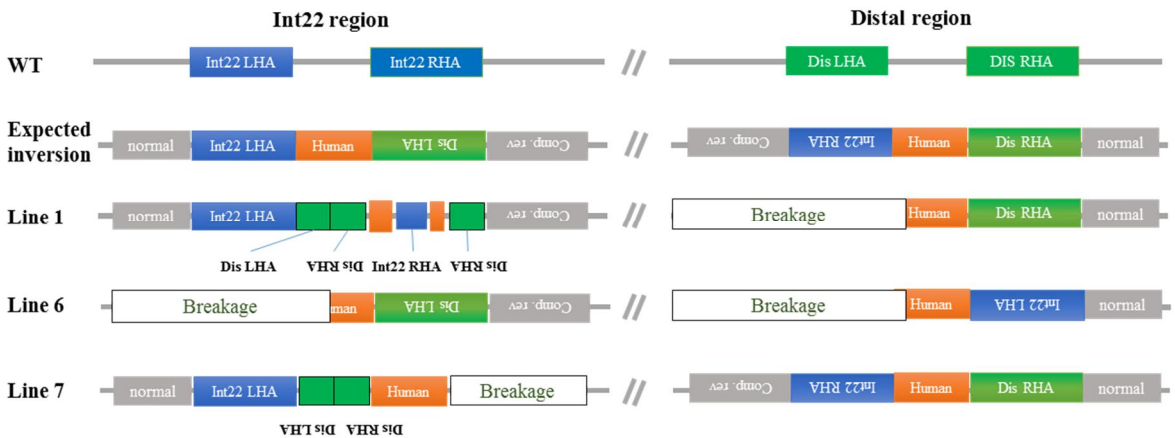

Figure 11. **Brief structure information of founder pups** we found inversion of *F8* in all three mutant founder pups. Human sequence for future re-inversion site is well inserted at inversion break site of both int22 and distal region. Partial degradation was observed one side of inversion break site.

#1 and #7 founder mice exhibited blood clotting disorder

Clotting disorder was evaluated by in vivo bleeding test, and founder line #1 and #7 exhibited blood clotting disorder. Even mutant mice from line #1 only developed significant different blood loss ($p = 0.0018$) (Figure 12), but line #7 mice also showed relatively large blood loss pattern than control. The average blood loss per body weight (mg/g) were 0.83 in control mice, 6.90 in line #1, 1.66 in line #6, and 3.02 in line #7 mice. Individual measure value is shown in table 9. After genetic rearrangement of each founder line, F8 protein expression was examined by immunohistochemistry. As shown in Figure 13, wild type B6 mice expressed F8 in liver, but all produced mutant mice did not exhibit F8 expression. This indicates that all founder mice were successfully established as inversion meditated hemophilia A mouse model.

Taken together, mouse line #7 were selected as candidate for further in vivo gene correction via AAV-CjCas9-sgRNA. As shown in Figure 14, #7 founder mouse showed precise knock in of human sequence in distal region, and this indicate that re-inversion would develop precise intron 22 region repair and re-gain of F8 function.

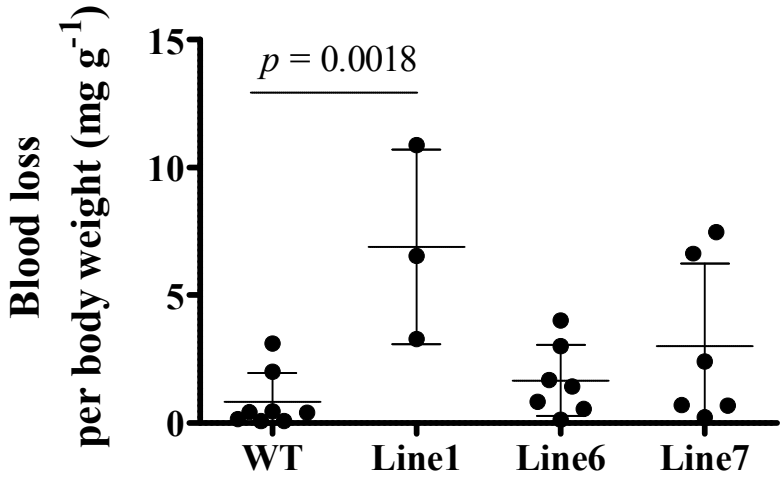

Figure 12. *in vivo* bleeding test with F2 mutant mice from 3 different founders. Each dot indicated measured value of blood loss per body weight. *p* value was calculated with student *t* test. Among 3 types of mutant, line1 and line7 mice showed high blood loss, compared to control group.

Table 9. Detail information about in vivo bleeding test with F2 mutant male mice from 3 different line

Mouse Type	No	Sex	Age (days)	Mouse weight(g)	Amount of blood loss (mg)	Blood loss per body weight (mg g-1)
WT	1188	M	89	26.9	**11**	0.408922
	1189	M	61	26.0	**2**	0.076923
	1190	M	89	28.9	**12**	0.415225
	1191	M	89	26.2	**4**	0.152672
	1192	M	89	30.4	**2**	0.065789
	1202	M	73	24.29	**11**	0.452861
	1203	M	53	22.77	**71**	3.118138
	1204	M	53	20.45	**41**	2.00489
Line 1	1193	M	42	20.86	**227**	10.88207
	1194	M	42	20.32	**67**	3.297244
		M	46	20.96	**137**	6.53626
Line 6	1195	M	89	30.57	**92**	3.009486
	1196	M	89	28.82	**41**	1.422623
	1197	M	89	29.86	**4**	0.133958
	1198	M	89	31.54	**53**	1.680406
	1205	M	73	23.12	**93**	4.022491
	1206	M	73	24.11	**20**	0.829531
	1207	M	53	22.31	**12**	0.537875
Line 7	1199	M	63	32.07	**77**	2.400998
	1200	M	63	28.91	**20**	0.691802
	1201	M	61	24.96	**17**	0.68109
	1208	M	52	26.2	**196**	7.480916
	1209	M	52	23.09	**153**	6.626245
	1210	M	47	23.25	**5**	0.215054

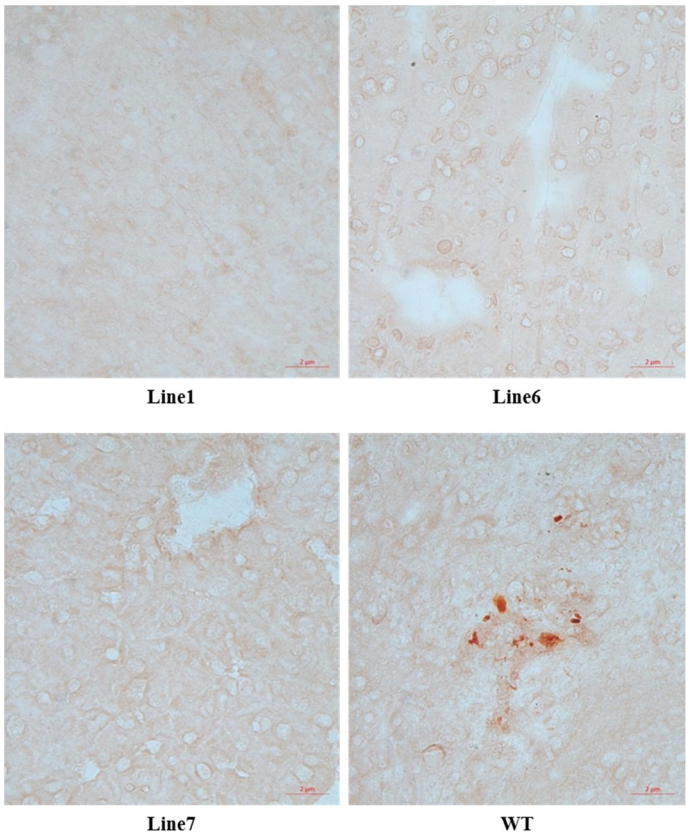

Figure 13.Confirmation of the absence of F8 expression in the liver of the inv22 mutant mice by Immunohistochemistry. Liver tissues from each mutant line were fixed and immunohistochemistry was conducted with rabbit anti-F8 antibody. Every mutant mice did not express F8 protein in liver tissue, but only control B6 mice express F8 (400x).

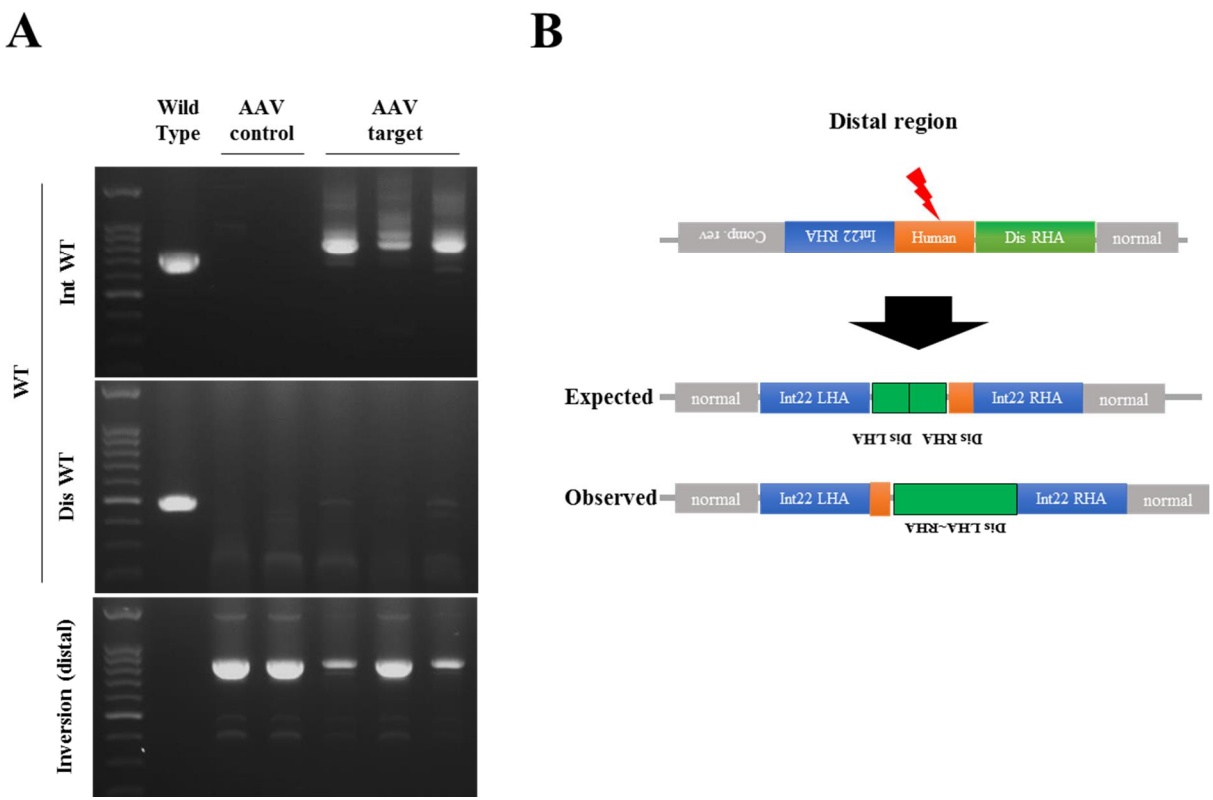

Figure 14. AAV mediated re-inversion in mutant MEF. A) With MEF from founder line #7, AAV transduction was conducted, and re-inversion was analyzed by PCR. Only AAV-Cjcas9 for target developed re-inversion, B) Brief DNA structure for positive clone of re-inversion.

Evidence of re-inversion by AAV-CjCas9 in mouse fetal fibroblast cell

For confirming the possibility of re-inversion meditated gene correction via AAV, fetal fibroblast cell from founder line #7 were established. Briefly, 4 MEF were successfully established, and 2 mutant male cells were identified by PCR method (Figure 15). They exhibited same gene amplification pattern with founder #7 mouse. After MEF preparation, AAV-CjCas9-sgRNA and control AAV-CjCas9 were transduced, and evidence of re-inversion were evaluated by PCR and sequencing. Only AAV-CjCas9-sgRNA developed re-inversion like sequence, but no control treatment group did not. The amplicon size of AAV-CjCas9-sgRNA were slightly larger than wild type control. This would be caused by inserted human sequence (Figure 15A). For verifying exact NHEJ mediated re-inversion by AAV, additional sequencing analysis was conducted. As shown in Figure 15B, there were re-inversion sequence in intron22 region, and also, indel of human sequence were observed. Even though DNA structure of observed int22 inversion region sequence were slightly different with our expectation, these results could be strong evidence of AAV-CjCas9-sgRNA mediated re-inversion.

Possibility of in vivo re-inversion by AAV-CjCas9 in mutant mouse

Next, *in vivo* AAV transduction for re-inversion mediated gain of function, male mutant mice from founder line #7 were selected, and treated AAV-CjCas9-sgRNAs and AAV-CjCas9 control. Even though the total number of tested mice were small, but there were remarkable change of blood loss volume between treat and control mice. AAV-CjCas9control mice exhibited about 10 mg/g of blood loss, but AAV-CjCas9-sgRNA mice only 2 mg/g of blood loss (Figure 16). There were still need for repeated test confirming the possibility of AAV mediated in vivo gene correction.

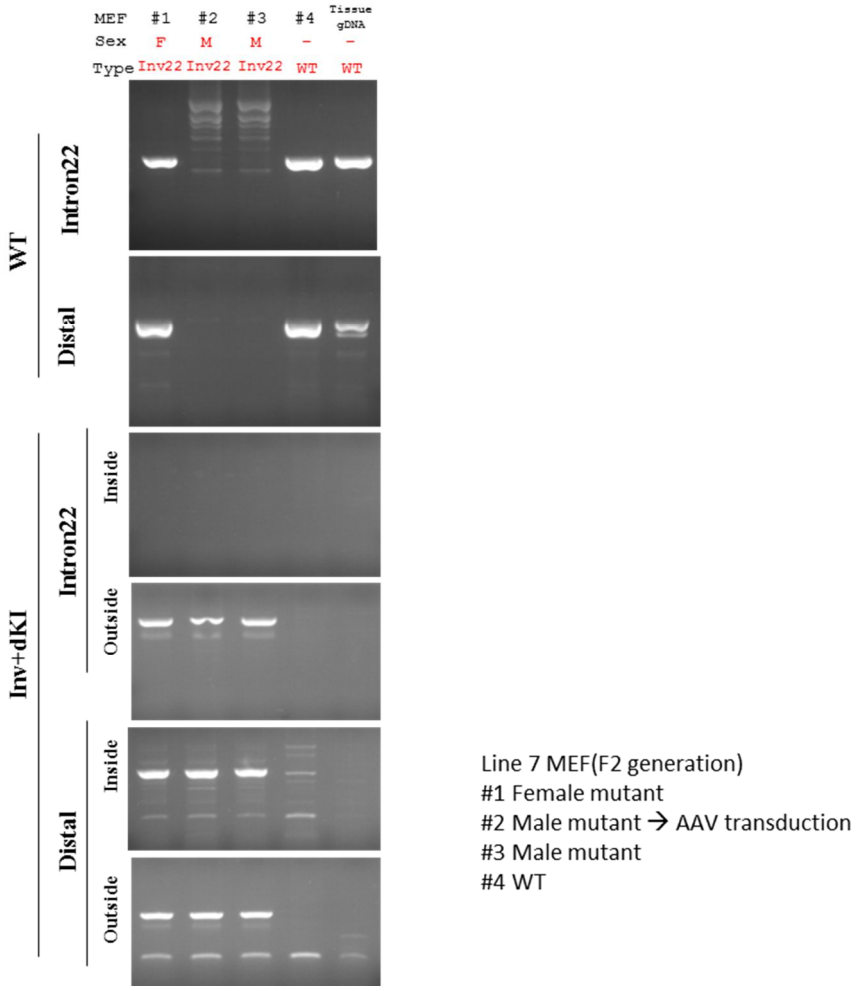

Figure 15. Preparation of MEF from founder line #7. MEF cells were established from 4 fetus, and it were genotyped by using PCR.MEF#1 was determined as Hu-inv22 based heterozygous female. MEF#2 was determined as Hu-inv22 based hemizygous male. MEF#3 was identified as Hu-inv22 based hemizygous male. MEF#4 was identified as WT. PCR products from WT tissue DNA were used as control.

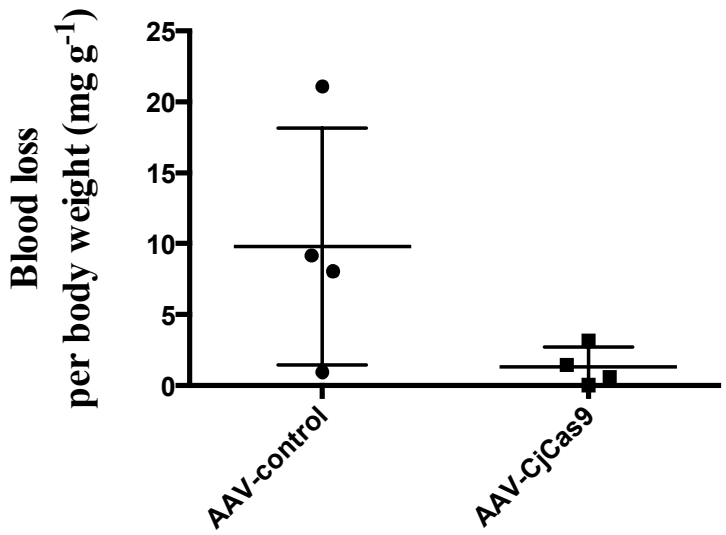

Figure 16. *in vivo* AAV-Cjcas9 mediated gene correction. *In vivo* bleeding test was conducted for AAV-CjCas9-sgRNA and AAV-CjCas9 control injected mutant mice (male and founder line #7). Each dot indicates that value from individual mice. Bleeding phenotype was observed in AAV-control treated mutant mouse, while meliorated bleeding phenotype was found in AAV-CjCas9 treated mutant mouse.

Discussion

CRISPR/Cas9 is a simple and efficient tool to edit genomes[33],[34]. Due to its simplicity and efficiency, CRISPR/Cas9 has been extended into various disease animal modeling. Although human disease is caused by many types of variants such as indel, duplication, large deletion, translocation, inversion, or copy number variant (CNV), so far, most of disease animal models have been designed through indel-based gene disruption. This limited animal modeling is caused by the idea that SV is difficult to be induced. Recent studies showed various SV such as inversion, large deletion, and duplication can be generated by using NHEJ pathway.[14, 35, 36] Another studies showed SV can be generated by using HDR pathway by inducing DSB in DNA sequence present at nonalleic locus with high similarity.[14, 37] This method is based on the mechanism that DSB can be repaired by homologous sequence. On the basis of this mechanism, DSB event in intra-palindrome sequence can induce intrachromatid genomic rearrangement resulting in inversion.

In this study, I showed generation of inversion based hemophilia A mice model, which is typical inversion-derived coagulation disorder in human, by using novel strategy. This novel method is based on inducing knock in by introducing ssODNs, guiding chromosomal segment in inverted orientation. To mimic *de novo* inversion, two genomic regions were targeted with sgRNAs, and made it jointed in inverted orientation with guiding ssODN. Compared to NHEJ-mediated inversion (5%)[36], HDR-mediated inversion (0.4%)[14] in previous studies, this novel method can generate inversion successfully at high rates (53.8%).

To induce inversion efficiently, Firstly, concurrent DSB should be ensured. Hence,

sgRNAs' cleavage potency were tested in NIH3t3cell, by transfecting Cas9 and sgRNA plasmid. Some sgRNA candidates showed high cleavage potency, while the others showed low cleavage potency. In general, prediction of potential sgRNA is made by sgRNA prediction tools, based on sgRNA length, PAM, GC rates, G-quadruplex, and CpG island. However, empirically, this prediction doesn't ensure cleavage all the time. It is believed that some unfound factor may contribute to sgRNA potency. For this reason, sgRNAs potency were assessed in NIH3T3 cells, and selected 3 sgRNAs for each target site, based on indel efficiency. Subsequently, to maximize concurrent DSB, Efficiency of Cas9 plasmid and Cas9 mRNA was tested in embryo microinjection. Cleavage efficiency was evaluated by whether NHEJ occur or not. Both Cas9 mRNA and Cas9 protein showed similarly high efficiency in embryo. Generally, Cas9 protein is more efficient in embryo manipulation, owing to time, required to express Cas9 protein from plasmid. However, in this data, efficiency of Cas9 mRNA and Cas9 protein was almost similar. Cas9 mRNA was chosen in this experiment, due to technical difficulty in microinjection caused by stickiness of protein. To seek optimal inversion condition in embryo, inversion efficiency between microinjection group with Cas9 mRNA, sgRNAs, ssODN, and group of Cas9 mRNA, sgRNAs was evaluated. In embryo, group with guiding ssODN showed threefold inversion efficiency (43.8%) than group without guiding ssODN (13.0%). Furthermore, as I designed ssODN to contain human sequence, human sequence knock-in in mouse embryo was also confirmed by using PCR with proper primers. After verification of int22 inversion in embryo, I generated int22 inversion based humanized HA mice, using above verified condition. To confirm genomic rearrangement, inversion junction site was amplified by using proper primers. Genotyping result indicated that not only 3 types of inversion mouse, but also large deletion mouse was obtained. Hemophilic phenotype in inversion mouse was confirmed by performing *in vivo* bleeding test. Absence of

F8 expression in the liver of the inversion mouse was confirmed by Immunohistochemistry, which suggests that inverted F8 protein might have low F8 expression level or instability. As I generated inversion based HA mouse successfully with human sequence in inversion junction site, this Hu-inv22 mouse model can be applicable in biological test, and pre-clinical test of HA.

After successful generation of Int22 inversion-based humanized mouse, I attempted correction of inversion-based HA by using AAV. To evaluate feasibility of gene correction by using AAV, AAV mediated re-inversion was tested in mutant MEF. As a result, gene correction was confirmed by amplifying re-inversion-derived WT F8. Based on *in vitro* gene correction result, re-inversion of *F8* in int22 inversion-based humanized HA mouse was tested. Consequently, I observed meliorated bleeding phenotype in AAV-CjCas9-treated inversion mice, while AAV-control-treated inversion mice exhibited the same hemophilic phenotype. This results suggest that treatment of single AAV-CjCas9 can be an efficient method to induce *in vivo* inversion, and correct disease.

Interestingly, in this study, I showed inversion induced by concurrent DSB along with guiding ssODN is more efficient than NHEJ-mediated inversion and HDR-mediated inversion. However, sequence variant was also observed unexpectedly at the inversion junction site. This result make it difficult to be interpreted at first, because guiding ssODNs were employed in inversion to introduce knock-in based HDR. Considering breakage in inversion junction site, it can be speculated that non-allelic homologous recombination (NAHR) or microhomology-mediated end joining (MMEJ) may be associated in inversion.[38] This suggests that guiding ssODN facilitate inversion efficiently, while inversion along with precise knock-in would be difficult to be generated. This undefined repair pathway might also explain why one

side of inversion junction site was not amplified in PCR based genotyping.

In conclusion, I found that inversion can be induced efficiently through guiding ssODN-based repair pathway, and as shown in *in vitro, in vivo* test, AAV can be extended into correction of inversion derived disorder.

Reference

[1] Bowen DJ: Haemophilia A and haemophilia B: molecular insights. Mol Pathol 2002, 55:127-44.

[2] Gitschier J, Wood WI, Goralka TM, Wion KL, Chen EY, Eaton DH, Vehar GA, Capon DJ, Lawn RM: Characterization of the human factor VIII gene. Nature 1984, 312:326-30.

[3] Lenting PJ, van Mourik JA, Mertens K: The life cycle of coagulation factor VIII in view of its structure and function. Blood 1998, 92:3983-96.

[4] Gouw SC, van den Berg HM, Oldenburg J, Astermark J, de Groot PG, Margaglione M, Thompson AR, van Heerde W, Boekhorst J, Miller CH, le Cessie S, van der Bom JG: F8 gene mutation type and inhibitor development in patients with severe hemophilia A: systematic review and meta-analysis. Blood 2012, 119:2922-34.

[5] Gouw SC, Van Der Bom JG, Van Den Berg HM, Zewald RA, Ploos Van Amstel JK, Mauser-Bunschoten EP: Influence of the type of F8 gene mutation on inhibitor development in a single centre cohort of severe haemophilia A patients. Haemophilia 2011, 17:275-81.

[6] Nielsen LN, Wiinberg B, Hager M, Holmberg HL, Hansen JJ, Roepstorff K, Tranholm M: A novel F8 -/- rat as a translational model of human hemophilia A. J Thromb Haemost 2014, 12:1274-82.

[7] Booth CJ, Brooks MB, Rockwell S, Murphy JW, Rinder HM, Zelterman D, Paidas MJ, Compton SR, Marks PW: WAG-F8(m1Ycb) rats harboring a factor VIII gene mutation provide a new animal model for hemophilia A. J Thromb Haemost 2010, 8:2472-7.

[8] Graham JB, Buckwalter JA, et al.: Canine hemophilia; observations on the course, the clotting anomaly, and the effect of blood transfusions. J Exp Med 1949, 90:97-111.

[9] Lozier JN, Dutra A, Pak E, Zhou N, Zheng Z, Nichols TC, Bellinger DA, Read M, Morgan RA: The Chapel Hill hemophilia A dog colony exhibits a factor VIII gene inversion. Proc Natl Acad Sci U S A 2002, 99:12991-6.

[10] Hough C, Kamisue S, Cameron C, Notley C, Tinlin S, Giles A, Lillicrap D: Aberrant splicing and premature termination of transcription of the FVIII gene as a cause of severe canine hemophilia A: similarities with the intron 22 inversion

mutation in human hemophilia. Thromb Haemost 2002, 87:659-65.
[11] Kashiwakura Y, Mimuro J, Onishi A, Iwamoto M, Madoiwa S, Fuchimoto D, Suzuki S, Suzuki M, Sembon S, Ishiwata A, Yasumoto A, Sakata A, Ohmori T, Hashimoto M, Yazaki S, Sakata Y: Porcine model of hemophilia A. PLoS One 2012, 7:e49450.
[12] Porada CD, Sanada C, Long CR, Wood JA, Desai J, Frederick N, Millsap L, Bormann C, Menges SL, Hanna C, Flores-Foxworth G, Shin T, Westhusin ME, Liu W, Glimp H, Zanjani ED, Lozier JN, Pliska V, Stranzinger G, Joerg H, Kraemer DC, Almeida-Porada G: Clinical and molecular characterization of a re-established line of sheep exhibiting hemophilia A. J Thromb Haemost 2010, 8:276-85.
[13] Bi L, Lawler AM, Antonarakis SE, High KA, Gearhart JD, Kazazian HH, Jr.: Targeted disruption of the mouse factor VIII gene produces a model of haemophilia A. Nat Genet 1995, 10:119-21.
[14] Lee HJ, Kweon J, Kim E, Kim S, Kim JS: Targeted chromosomal duplications and inversions in the human genome using zinc finger nucleases. Genome Res 2012, 22:539-48.
[15] Lee HJ, Kim E, Kim JS: Targeted chromosomal deletions in human cells using zinc finger nucleases. Genome Res 2010, 20:81-9.
[16] Wu Y, Liang D, Wang Y, Bai M, Tang W, Bao S, Yan Z, Li D, Li J: Correction of a genetic disease in mouse via use of CRISPR-Cas9. Cell Stem Cell 2013, 13:659-62.
[17] Tabebordbar M, Zhu K, Cheng JKW, Chew WL, Widrick JJ, Yan WX, Maesner C, Wu EY, Xiao R, Ran FA, Cong L, Zhang F, Vandenberghe LH, Church GM, Wagers AJ: In vivo gene editing in dystrophic mouse muscle and muscle stem cells. Science 2016, 351:407-11.
[18] Park CY, Kim DH, Son JS, Sung JJ, Lee J, Bae S, Kim JH, Kim DW, Kim JS: Functional Correction of Large Factor VIII Gene Chromosomal Inversions in Hemophilia A Patient-Derived iPSCs Using CRISPR-Cas9. Cell Stem Cell 2015, 17:213-20.
[19] Fisher KJ, Jooss K, Alston J, Yang Y, Haecker SE, High K, Pathak R, Raper SE, Wilson JM: Recombinant adeno-associated virus for muscle directed gene therapy. Nat Med 1997, 3:306-12.
[20] Kessler PD, Podsakoff GM, Chen X, McQuiston SA, Colosi PC, Matelis LA, Kurtzman GJ, Byrne BJ: Gene delivery to skeletal muscle results in sustained expression and systemic delivery of a therapeutic protein. Proc Natl Acad Sci U S A 1996, 93:14082-7.

[21] Snyder RO, Miao CH, Patijn GA, Spratt SK, Danos O, Nagy D, Gown AM, Winther B, Meuse L, Cohen LK, Thompson AR, Kay MA: Persistent and therapeutic concentrations of human factor IX in mice after hepatic gene transfer of recombinant AAV vectors. Nat Genet 1997, 16:270-6.
[22] Xiao X, Li J, Samulski RJ: Efficient long-term gene transfer into muscle tissue of immunocompetent mice by adeno-associated virus vector. J Virol 1996, 70:8098-108.
[23] Kim E, Koo T, Park SW, Kim D, Kim K, Cho HY, Song DW, Lee KJ, Jung MH, Kim S, Kim JH, Kim JH, Kim JS: In vivo genome editing with a small Cas9 orthologue derived from Campylobacter jejuni. Nat Commun 2017, 8:14500.
[24] Astermark J, Petrini P, Tengborn L, Schulman S, Ljung R, Berntorp E: Primary prophylaxis in severe haemophilia should be started at an early age but can be individualized. Br J Haematol 1999, 105:1109-13.
[25] Oldenburg J: Optimal treatment strategies for hemophilia: achievements and limitations of current prophylactic regimens. Blood 2015, 125:2038-44.
[26] Evatt BL, Robillard L: Establishing haemophilia care in developing countries: using data to overcome the barrier of pessimism. Haemophilia 2000, 6:131-4.
[27] Nathwani AC, Reiss UM, Tuddenham EG, Rosales C, Chowdary P, McIntosh J, Della Peruta M, Lheriteau E, Patel N, Raj D, Riddell A, Pie J, Rangarajan S, Bevan D, Recht M, Shen YM, Halka KG, Basner-Tschakarjan E, Mingozzi F, High KA, Allay J, Kay MA, Ng CY, Zhou J, Cancio M, Morton CL, Gray JT, Srivastava D, Nienhuis AW, Davidoff AM: Long-term safety and efficacy of factor IX gene therapy in hemophilia B. N Engl J Med 2014, 371:1994-2004.
[28] Wang X, Seed B: A PCR primer bank for quantitative gene expression analysis. Nucleic Acids Res 2003, 31:e154.
[29] Graw J, Brackmann HH, Oldenburg J, Schneppenheim R, Spannagl M, Schwaab R: Haemophilia A: from mutation analysis to new therapies. Nat Rev Genet 2005, 6:488-501.
[30] Naumova AK, Plenge RM, Bird LM, Leppert M, Morgan K, Willard HF, Sapienza C: Heritability of X chromosome--inactivation phenotype in a large family. Am J Hum Genet 1996, 58:1111-9.
[31] Chao BN, Baldwin WH, Healey JF, Parker ET, Shafer-Weaver K, Cox C, Jiang P, Kanellopoulou C, Lollar P, Meeks SL, Lenardo MJ: Characterization of a genetically engineered mouse model of hemophilia A with complete deletion of the F8 gene. J Thromb Haemost 2016, 14:346-55.
[32] Zincarelli C, Soltys S, Rengo G, Rabinowitz JE: Analysis of AAV serotypes 1-9

mediated gene expression and tropism in mice after systemic injection. Mol Ther 2008, 16:1073-80.
[33] Cho SW, Kim S, Kim JM, Kim JS: Targeted genome engineering in human cells with the Cas9 RNA-guided endonuclease. Nat Biotechnol 2013, 31:230-2.
[34] Wang H, Yang H, Shivalila CS, Dawlaty MM, Cheng AW, Zhang F, Jaenisch R: One-step generation of mice carrying mutations in multiple genes by CRISPR/Cas-mediated genome engineering. Cell 2013, 153:910-8.
[35] Li J, Shou J, Guo Y, Tang Y, Wu Y, Jia Z, Zhai Y, Chen Z, Xu Q, Wu Q: Efficient inversions and duplications of mammalian regulatory DNA elements and gene clusters by CRISPR/Cas9. J Mol Cell Biol 2015, 7:284-98.
[36] Kraft K, Geuer S, Will AJ, Chan WL, Paliou C, Borschiwer M, Harabula I, Wittler L, Franke M, Ibrahim DM, Kragesteen BK, Spielmann M, Mundlos S, Lupianez DG, Andrey G: Deletions, Inversions, Duplications: Engineering of Structural Variants using CRISPR/Cas in Mice. Cell Rep 2015.
[37] Park CY, Kim J, Kweon J, Son JS, Lee JS, Yoo JE, Cho SR, Kim JH, Kim JS, Kim DW: Targeted inversion and reversion of the blood coagulation factor 8 gene in human iPS cells using TALENs. Proc Natl Acad Sci U S A 2014, 111:9253-8.
[38] McVey M, Lee SE: MMEJ repair of double-strand breaks (director's cut): deleted sequences and alternative endings. Trends Genet 2008, 24:529-38.

Abstract in Korean

혈우병A는 Factor8 이라는 단백질에서의 nonsense 돌연변이, missense 돌연변이, 작은 서열의 삽입이나 삭제, splice site 돌연변이, 큰 삭제, 역위와 같은 각종 돌연변이에 의해 일어난다. 특히 그 중 인트론22 역위 유래 혈우병A의 경우는 중증 혈우병 양상 환자의 절반 가까이를 차지한다. 하지만 역위 유래 혈우병A 같은 심각한 증상의 혈우병의 경우 inhibitor의 발달로 적절한 치료에 어려움을 겪고 있다. 이러한 이유 때문에 안전한 치료제 개발과 전임상 연구를 위해서는 동물질환모델이 필수적이다. 하지만 이러한 동물모델의 필요성에도 불구하고 지금까지 적절한 역위 유래 혈우병A 동물모델들은 잘 개발되지 못했다.

이번 연구에서는 CRISPR/Cas9이라는 genome engineering 시스템을 이용하여 유전적으로 역위를 일으킬 수 있다는 것을 보여주었다. 마우스 배아에서 Non-Homologous End Joining(NHEJ) 매개 역위는 13.1%의 효율을 보여줬으며, Homology Direct Repair(HDR) 매개 역위는 43.8%의 효율로 나타났다. 또한 HDR를 이용한 역위 마우스 제작에서도 53.8%라는 높은 효율을 나타내었다. 역위가 발생되는 절단 부위에서 약간의 서열변이가 관찰되었지만 역위 기반의 인간화 혈우병A 마우스는 성공적으로 만들어졌다. 이 마우스들에서는 간에서 F8 단백질의 결핍 그리고 과도한 출혈과 같은 혈우병A 관련 증상들을 관측할 수 있었다. 뿐만 아니라 더 나아가서 Mouse Embryonic Fibroblast(MEF)에서 (Adeno Associated Virus)AAV와 Campilobaccter jejuni Cas9(CjCas9)을 이용하여

인간화 마우스에서 사람의 유전자 서열을 타겟팅함으로써 역위된 F8을 재역위 할 수 있다는 것을 보여주었다. 이를 통하여 AAV-CjCas9이 structural variant (SV)인 inversion 모델의 치료에도 쓰일 수 있다는 것을 알 수 있었다. 이번 연구 결과는 인간화 역위 기반 혈우병 마우스가 역위 기반 혈우병의 다양한 연구에 쓰일 수 있을 것이라는 것을 보여주었고 AAV가 역위 기반 혈우병의 치료제로서 효과가 있다는 것을 보여주었다.

주요어 : 혈우병 A, 구조적 변이, 역위, 유전자 교정, 유전자 가위, Factor8

학 번 : 2016-20014